



Citation for published version:

Sarihan, A, Shahid, S, Shen, J, Amura, I, Patterson, DA & Emanuelsson, EAC 2019, 'Exploiting the electrical conductivity of poly-acid doped polyaniline membranes with enhanced durability for organic solvent nanofiltration', *Journal of Membrane Science*, vol. 579, pp. 11-21. <https://doi.org/10.1016/j.memsci.2019.02.030>

DOI:

[10.1016/j.memsci.2019.02.030](https://doi.org/10.1016/j.memsci.2019.02.030)

Publication date:

2019

Document Version

Peer reviewed version

[Link to publication](#)

Publisher Rights

CC BY-NC-ND

University of Bath

General rights

Copyright and moral rights for the publications made accessible in the public portal are retained by the authors and/or other copyright owners and it is a condition of accessing publications that users recognise and abide by the legal requirements associated with these rights.

Take down policy

If you believe that this document breaches copyright please contact us providing details, and we will remove access to the work immediately and investigate your claim.

1 **Exploiting the electrical conductivity of poly-acid doped polyaniline membranes with**
2 **enhanced durability for organic solvent nanofiltration**

3

4 Adem Sarihan^{1,2,3}, Salman Shahid^{1,2}, Junjie Shen^{1,2}, Ida Amura^{1,2}, Darrell Alec Patterson^{1,2},
5 Emma Anna Carolina Emanuelsson^{2,*}

6 ¹ Centre for Advanced Separations Engineering, University of Bath, Bath, United Kingdom,
7 BA2 7AY.

8 ² Department of Chemical Engineering, University of Bath, Bath, United Kingdom, BA2
9 7AY.

10 ³ Bilecik Vocational School, Bilecik Seyh Edebali University, Bilecik, Turkey, 11230

11

12

Submitted to

13

14

Journal of Membrane Science

15

16

17

18

19

20

21 *Corresponding author: E.A.Emanuelsson-Patterson@bath.ac.uk

22

23

24

25 **Abstract**

26 We have developed stable organic solvent nanofiltration (OSN) membranes that are electrically
27 conductive. These membranes overcome key issues with current tuneable membranes:
28 molecular weight cut off (MWCO) limited to the UF-range and lack of filtration stability.
29 Polyaniline (PANI) was in-situ doped by poly(2-acrylamido-2-methyl-1-propanesulfonic acid)
30 (PAMPSA) using chemical oxidative polymerisation that leads to formation of interpolymer
31 complex. The PANI-PAMPSA membranes were prepared by phase inversion method and the
32 pore sizes were shrunk by annealing the membranes at temperatures lower than the crosslinking
33 temperature. The membranes were systematically evaluated using visual and chemical analysis
34 and in-filtration experiments. The developed membranes were solvent stable, reusable, had a
35 denser structure and lower MWCO and there was no thermal crosslinking as seen by IR. The
36 solvent permeance obtained were: 0.46, 0.60 and 0.74 Lm⁻²h⁻¹bar⁻¹ for acetone, 2-propanol and
37 methanol respectively, with MWCO below 300 Da and 266 Da for methanol. For the
38 tuneability investigation, when applying an electrical potential (20 V) in a custom-made cross-
39 flow membrane cell, an increase in MWCO and permeance (10.4% and 55.6%, respectively)
40 was observed. These results show that this simple in-situ doping method with heat treatment
41 can produce promising and stable PANI membranes, for OSN processes in different solvents,
42 with the distinctive feature of in-situ performance control by applying external electrical
43 potential.

44 **Key words:** Polyaniline, Organic solvent nanofiltration, Electrical tuneable membranes, Heat
45 treatment

46 **1. Introduction**

47 Organic solvent nanofiltration (OSN), also known as solvent resistant nanofiltration [1] can
48 separate materials with molecular weight between 200-1000 Da present in organic solvents [2,
49 3, 4, 5]. It has several advantages in comparison to conventional temperature based methods,
50 including low energy consumption and ease to integrate in existing processes [2, 3, 5, 6]. OSN
51 has the potential to become the best available technology among the separation techniques in
52 organic media [4] for a wide range of processes related to, e.g. food [7-9], fine chemical [10,
53 11], pharmaceutical [12, 13] and petrochemical industries [14, 15]. The main limitations with
54 existing OSN membranes are limited solvent and filtration stability and fouling. Membranes
55 that change the permeance and MWCO during filtration (tuneable membranes) could change

56 their transport properties and allow for in-situ self-cleaning/fouling removal, therefore
57 changing the pore size during filtration has the potential to overcome fouling. To the best
58 knowledge of the authors, there are no OSN membranes that have tuneable properties.

59 To achieve tuneability, materials are prepared to respond to external stimuli, such as pH [16,
60 17], ionic strength [18], temperature [19], light [20], electricity [21] etc. Among these,
61 electrical tuneability offer the advantage that it can easily and quickly be applied to the
62 membrane [22]. To obtain electrical tuneability, the material must be able to undergo an
63 electrical change. Polyaniline (PANI) is a widely used polymer [23-28] that become conductive
64 through acid doping [21, 29]. Small acid dopants, like HCl, do leach out during filtration [30]
65 and therefore change the performance characteristics, including loss of electrical conductivity
66 [31] and make the membranes brittle [22]. Our research group has recently shown that
67 polymeric acids, poly(2-acrylamido-2-methyl-1-propanesulfonic acid) (PAMPSA), can
68 overcome the above disadvantages, possibly due to steric effects and the strong interaction
69 between the acidic group of the polymeric acids and the PANI. Although the membranes were
70 conductive and tuneable, the MWCO was in the UF-range and they had low filtration stability
71 [31].

72 Heat treatment is one of the simplest and cheapest post-treatment processes to both (i) shrink
73 the pores to obtain nanofiltration (NF) MWCO [32] and (ii) to improve filtration stability [27,
74 32, 33] as there is no need for chemicals like solvents and cross-linkers etc. However, the
75 thermal crosslinking occurs on the imine nitrogen of PANI [33, 34] which act as carriers of the
76 electric charge [35], reducing or losing the conductivity [32]. In addition, heat treatment also
77 result in significant reductions in permeance, with no permeance for certain solvents [33]. To
78 date, the crosslinking of PANI has been performed at comparatively high temperatures because
79 the thermal transition of the PANI occurs at 180 °C [24, 27, 34, 36 - 39]. We hypothesise, in
80 difference, that we can shrink the membrane pores at a lower temperature and thus achieve NF
81 membranes with conductivity properties, without having thermal crosslinking. This would
82 reduce the energy consumption and fine-tune the porosity of the membranes. We also
83 hypothesise, that these membranes will have improved solvent stability due to producing
84 denser and more compact membranes, further widening the application in OSN.

85 Therefore the aim of this study is to prepare novel, electrically tuneable and stable OSN
86 membranes with PAMPSA as a dopant for PANI by using heat treatment at temperatures lower

87 than the crosslinking temperature (110-130°C and 1-15h), to tighten the pores without
88 crosslinking. The physical, chemical and electrical properties of the membranes will be
89 evaluated using SEM, AFM, FTIR, dynamic contact angle goniometry and four-point probe
90 conductivity techniques. Solvent stability and swelling degrees of the heat treated membranes
91 will be investigated in a range of solvents with different polarity and compared to untreated
92 membranes. Rejection studies, MWCO determinations and electrically tuneability properties
93 will be performed using dead-end and cross-flow filtration techniques.

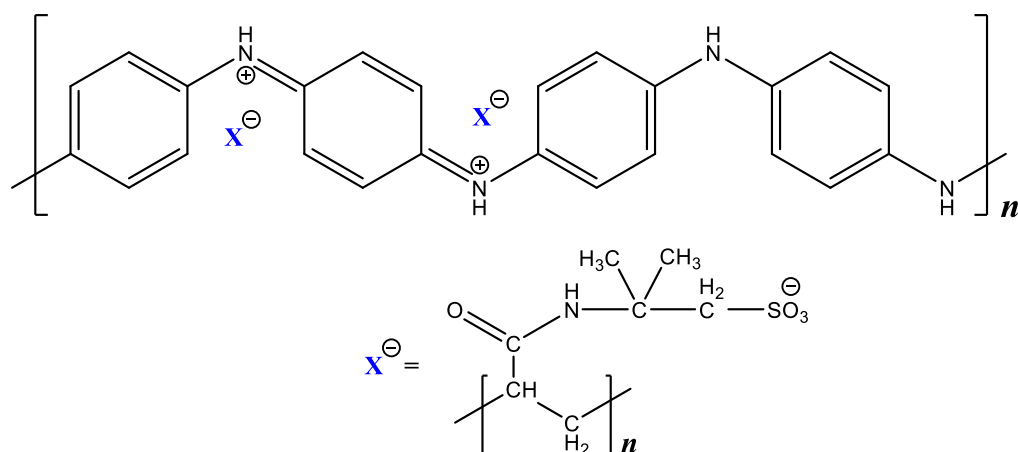
94 **2. Experimental**

95 **2.1. Materials**

96 Aniline, Poly (2-acrylamido-2-methyl-1-propanesulfonic acid) (PAMPSA, ammonium
97 persulfate (APS), 4-methyl piperidine (4MP), N-methyl-2-pyrrolidone (NMP) were obtained
98 from Sigma-Aldrich, UK and used to synthesize the PANI-PAMPSA as monomer, dopant
99 chemical oxidant, gel inhibitor and solvent for membrane casting solution, respectively. HPLC
100 grade toluene, n-hexane, acetone, isopropanol and methanol were supplied by Fisher Scientific
101 and used as solvents, UK. Tripropylene glycol and poly(propylene) glycols (PPGs, MW = 400,
102 725 and 1000 g mol⁻¹), were purchased from Alfa Aesar and used for MWCO determination
103 of prepared membranes. The non-woven polyethylene/polypropylene (PE/PP) mixture
104 membrane support layer (Novatexx 2431) was supplied by Freudenberg Filter, Germany.
105 Deionized (DI) water was produced by an ELGA deioniser from PURELAB Option, USA.

106 **2.2. Synthesis of PANI-PAMPSA polymer**

107 PANI-PAMPSA powder was synthesized by oxidative polymerization of aniline in PAMPSA.
108 0.2 mol of aniline and 0.05 mol of PAMPSA was used to prepare a solution in water (Solution
109 1). 0.2 mol of APS was dissolved in a second water bottle (Solution 2). Solution 2 was slowly
110 added into the aniline solution by a peristaltic pump at a speed of 20 mL h⁻¹, temperature was 15
111 °C, t for 24 h for complete polymerization. The obtained PANI-PAMPSA was filtered and
112 washed firstly with DI water 3 times and then with acetone 3 times until the pH of the filtrate
113 became neutral to remove the PANI oligomers and then dried in a vacuum oven at 65 °C for
114 24 h. Finally, the powder was grinded in mortar and a dark green product was obtained. The
115 chemical structure of the PANI-PAMPSA can be seen in Figure 1.



116

117 **Figure 1.** Chemical structure of the PANI-PAMPSA polymer (in Figure, $X^- = \text{PAMPSA}$).

118 2.3. Preparation and heat treatment of PANI-PAMPSA membranes

119 The PANI-PAMPSA membranes were prepared using non solvent induced phase inversion
 120 process [40, 41]. For the preparation of membrane casting solution, firstly NMP (solvent) and
 121 4-MP (gel inhibitor) and stirred for 5 minutes than appropriate amount of PANI-PAMPSA
 122 powder was added to solution slowly to get a 20% (w/w) PANI-PAMPSA. Then the mixture
 123 is stirred 24h to obtain a homogeneous solution. After 24h, the solution was left at least two
 124 hours at room temperature and put it in vacuum oven at 40 °C for 30 minutes to remove all the
 125 bubbles/air traps in it. The solution was then casted on the polyethylene/polypropylene (PE-
 126 PP) backing layer to make a 200 μm thick film using an adjustable casting knife (4340
 127 Automatic Film Applicator, Elcometer, UK) and then the film was immediately fully immersed
 128 into a coagulation bath containing DI water. The phase inversion occurred in the coagulation
 129 bath forming the membrane. The obtained membranes was left in pure water to wait until test
 130 or treatment.

131 To shrink/tighten the pores and to get dense structure to obtain nanofiltration range membranes,
 132 the prepared membranes were heat treated as different temperatures and times (see Table 1).
 133 Overall the heat treatment that applied in this study were between 1-3 hours (only for 110 °C
 134 it was tested for 15h to check the longer time heat treatment effect on membrane).

135

136

137 **Table 1.** Heat treatment conditions of PANI-PAMSA membranes

Temperature (°C)	Time (h)
110	1
110	2
110	15
120	1
120	2
120	3
130	1

138 For the heat treatment process, the membranes were cut to suitable size disks for dead-end cell
139 (14.6 cm²) and the disks were placed between two glass plates to prevent curling. The heat
140 treatment was performed in a vacuum oven (Thermo Scientific, VT 6025). After heat treatment,
141 membranes were placed in water until filtration tests.

142 **2.4. Fourier Transform Infrared Spectroscopy (FTIR) analysis**

143 Fourier transform infrared (FT-IR) spectrometer with an attenuated total reflectance (ATR) cell
144 (Spectrum 100, PerkinElmer, USA) was used to determine the chemical compositions of the
145 untreated and heat treated PANI-PAMPSA membranes. A background scan was run prior to
146 sample testing and spectra were recorded from 4000 to 650 cm⁻¹ but it was focussed especially
147 2000-1000 cm⁻¹.

148 **2.5. Scanning electron microscopy (SEM) and Atomic force microscopy (AFM) analysis**

149 The morphological properties of the membranes were investigated by a scanning electron
150 microscopy (SEM) (JSM-6480LV, JEOL, Japan). The samples were prepared by breaking
151 them in liquid nitrogen to obtain a smooth cross-section and then mounted on the SEM stubs
152 by conductive double-sided tape and dried overnight. The samples were coated with gold under
153 argon flow to reduce sample charging under the electron beam. Then the surface and cross-
154 section images were recorded in different magnification ranges.

155 Atomic force microscopy (AFM) were used to investigate the membrane roughness structure.
156 AFM images were taken by using Veeco multimode Nanoscope III microscopy. Besides the
157 AFM images of the membranes, mean roughness (Ra) that is the arithmetic average of the
158 absolute values of the roughness profile ordinates and root mean square roughness (Rq) that is
159 the root mean square average of the roughness profile ordinates were used to examine the
160 roughness.

161 2.6. Dynamic contact angle analysis

162 The dynamic contact angle analysis were performed by use of a contact angle goniometer
163 (Contact Angle System OCA 15Pro, Dataphysics, Germany). The membrane sample was
164 placed on an analytical platform a small drop of water (2 μ L) was placed onto the membrane
165 surface. A video camera was used to record images of the water drop. The programme software
166 was used to calculate the effective contact angle change on the membrane surface. The dynamic
167 contact angle analysis were repeated at least three times for all tested membranes.

168 2.7. Swelling and stability tests

169 For the swelling tests, the untreated and heat treated PANI-PAMPSA membranes were cut into
170 small samples (2cm \times 2cm) and dried in a vacuum oven. The mass of the dried membranes
171 were determined and the membranes put into the solvents in a sealed flask at 25 $^{\circ}$ C for 1 h.
172 The swollen membranes were taken from the solvent and quickly dried with a filter paper to
173 remove solvent from the external surface. The mass of the swollen membranes was then
174 determined. The mass swelling degree (Q_m) was calculated by using equation 1:

$$175$$
$$176 Q_m = \frac{m_{wet} - m_{dry}}{m_{dry}} \quad (1)$$

177 Where m_{wet} and m_{dry} is the mass of the wet and dry membranes, respectively.

178 The stability of the PANI-PAMPSA membranes in the solvents were determined by immersing
179 the membrane sample in the solvents for one week using the same conditions as the swelling
180 test. The mass change of the dry membrane before and after soaking in the solvent indicated
181 whether the membrane did dissolve in the certain solvent or not. Membrane stability (%S) was
182 calculated by using equation 2:

$$183$$
$$184 \%S = \frac{W_1 - W_2}{W_1} \times 100 \quad (2)$$

185

186 Where W_1 and W_2 are the dry weights of the membrane before and after soaking in the solvent
187 for one week

188 Water, Methanol, 2-propanol, acetone, toluene and hexane were chosen as different polarity
189 solvents to investigate the swelling and stability properties. The swelling and stability test was

190 repeated three times for each membrane. In addition, to investigate the stability during
191 filtration, a 24 hour (8 hour per solvent) filtration stability tests was performed using 2-
192 propanol, methanol and acetone under 20 bar pressure for the 120 °C 3h heat treated membrane.

193 **2.8. Nanofiltration tests and MWCO determinations**

194 The filtration tests of untreated and heat treated membranes were performed by using a stirred
195 high pressure stainless steel dead-end filtration cell (HP 4750, Sterlitech, USA). The pressure
196 applied was dependent on the membrane structure, for untreated PANI-PAMPSA membrane 1
197 bar was used. However, for the heat treated ones, 20 bar was required to obtain appropriate
198 permeance. The membranes were firstly preconditioned with solvents until obtaining a constant
199 permeance. Then rejection studies were performed with feed solutions using different
200 molecular weight of PPGs in the solvents (methanol, 2-propanol and acetone were chosen for
201 the nanofiltration tests). The MWCO of membrane is the MW of the solute molecule that gives
202 a 90% rejection [42]. Detailed information about the MWCO determination method used in
203 this study is described elsewhere [43]. The analysis of the PPG solution feed and permeate
204 were performed with high-performance liquid chromatography (HPLC) equipped with
205 evaporative light scattering detector (ELSD) (1260 Infinity, Agilent Technologies, USA).
206 Permeance and rejection results were calculated with equations 3 and 4, respectively.

$$207 \quad P = \frac{V}{A t p} \quad (3)$$

$$208 \quad R(\%) = \left(1 - \frac{C_p}{C_f}\right) \times 100 \quad (4)$$

209 Where V , A , t , p , C_p and C_f refers to volume (L), membrane effective area (m²), time (h),
210 pressure, permeate concentration and feed concentration, respectively.

211 **2.9. Conductivity, cross-flow filtration and tuneability studies**

212 The electrical conductivity of untreated and heat treated membranes were measured using a
213 four-point multi height probe (RM3000, Jandel Engineering Limited, UK) at room
214 temperature. The electrical conductivity was calculated as the reciprocal of electrical
215 resistivity. Sheet resistivity (ρ) is calculated by using Equation 5.

$$216 \quad \rho = 4.532 \times V \times \frac{t}{l} \quad (5)$$

217 Where ρ is resistivity, V is the measured electrical potential, I is the provided electrical current,
218 and t is the membrane thickness. Conductivities the inverse of resistivity ($1/\rho$).

219 The tuneability studies of the PANI-PAMPSA nanofiltration membranes were performed with
220 a custom-made electrically connected cross-flow filtration setup [22]. In a typical experiment,
221 PANI-PAMPSA membrane was placed in the cross-flow membrane cell and 1.5 L of PPG feed
222 solution in solvent was used in the reservoir tank. Permeates were collected at a constant
223 pressure of 20 bar and the flow rate was adjusted to 0.8 L min^{-1} during the experiment. Different
224 electrical potentials (0, 5, 10 and 20 V) were applied for the testing of the electrical tuneability
225 of membranes. Then the MWCOs and permeances of the membranes were determined for the
226 different potential applying filtrations. Methanol was chosen for cross-flow tuneability studies
227 as solvent because the exact MWCO value of the membrane can be determined in this solvent.

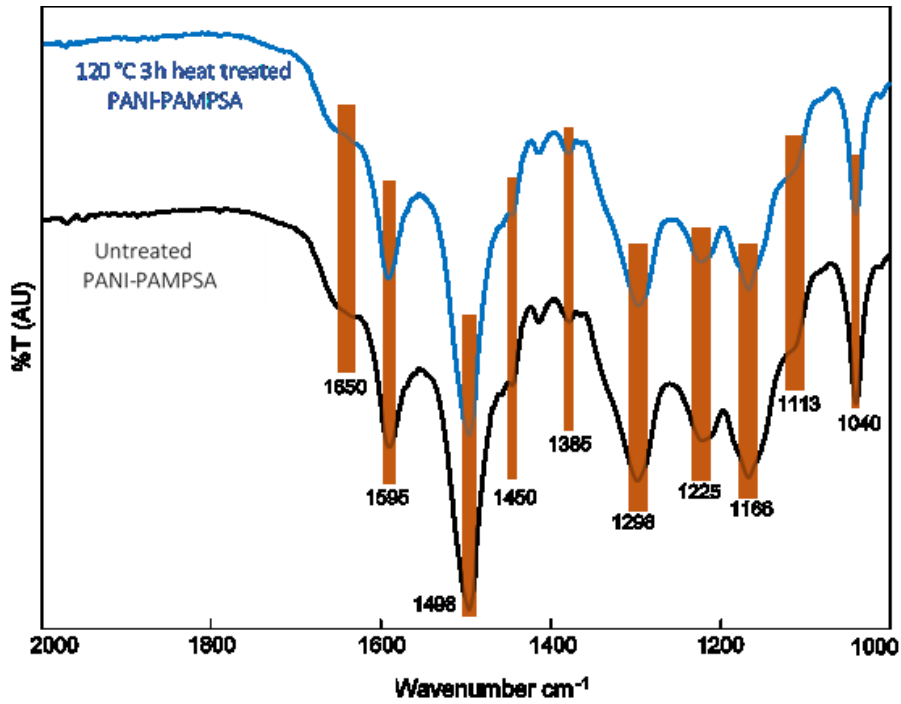
228 **3. Results and discussion**

229 **3.1. Fourier Transform Infrared Spectroscopy (FTIR) analysis**

230 Figure 2 shows the FTIR spectra of the untreated and the 120°C 3h heat treated PANI-
231 PAMPSA membrane (as a representative heat-treated membrane). The orange columns
232 represent peak widths. The absorption bands at approximately 1225-1113 and 1040 cm^{-1}
233 correspond to the asymmetric and symmetric stretching of $-\text{SO}_2-$ in the PAMPSA, respectively
234 [44, 45]. The peak at 1166 cm^{-1} could be assigned to the vibrational band of the nitrogen
235 quinone on the PANI [44, 46]. At 1298 cm^{-1} , the C-N stretch of a secondary aromatic amine
236 from the PANI was observed and the characteristic absorption peaks at 1595 cm^{-1} and 1498
237 cm^{-1} could be assigned to the stretches of the quinone and benzene ring from PANI,
238 respectively [44]. The C=O stretch band in the PAMPSA is shown near to 1660 cm^{-1} [52].
239 Finally, the methyl groups of PAMPSA give rise to absorption bands at 1450 and 1385 cm^{-1}
240 [45]. Confirming that the obtained polymer is PANI-PAMPSA. In addition, there is no
241 significant difference between the two FTIR spectra showing that there is no chemically
242 difference (crosslinking etc.) between the two membranes. If crosslinking had occurred, the
243 secondary amine band would be much smaller due to the formation of tertiary amines [27] and
244 the width of the peaks would have increased because of the increased interaction of the
245 vibrational modes due to physical chain crosslinking [47]. In summary, the heat treatment did
246 not cause any crosslinking, but caused some physical changes that was also observed in other

247 characterization results like SEM, AFM etc. See the supplementary materials (Fig S3) for the
248 infrared spectra of the other heat treated membranes.

249



250

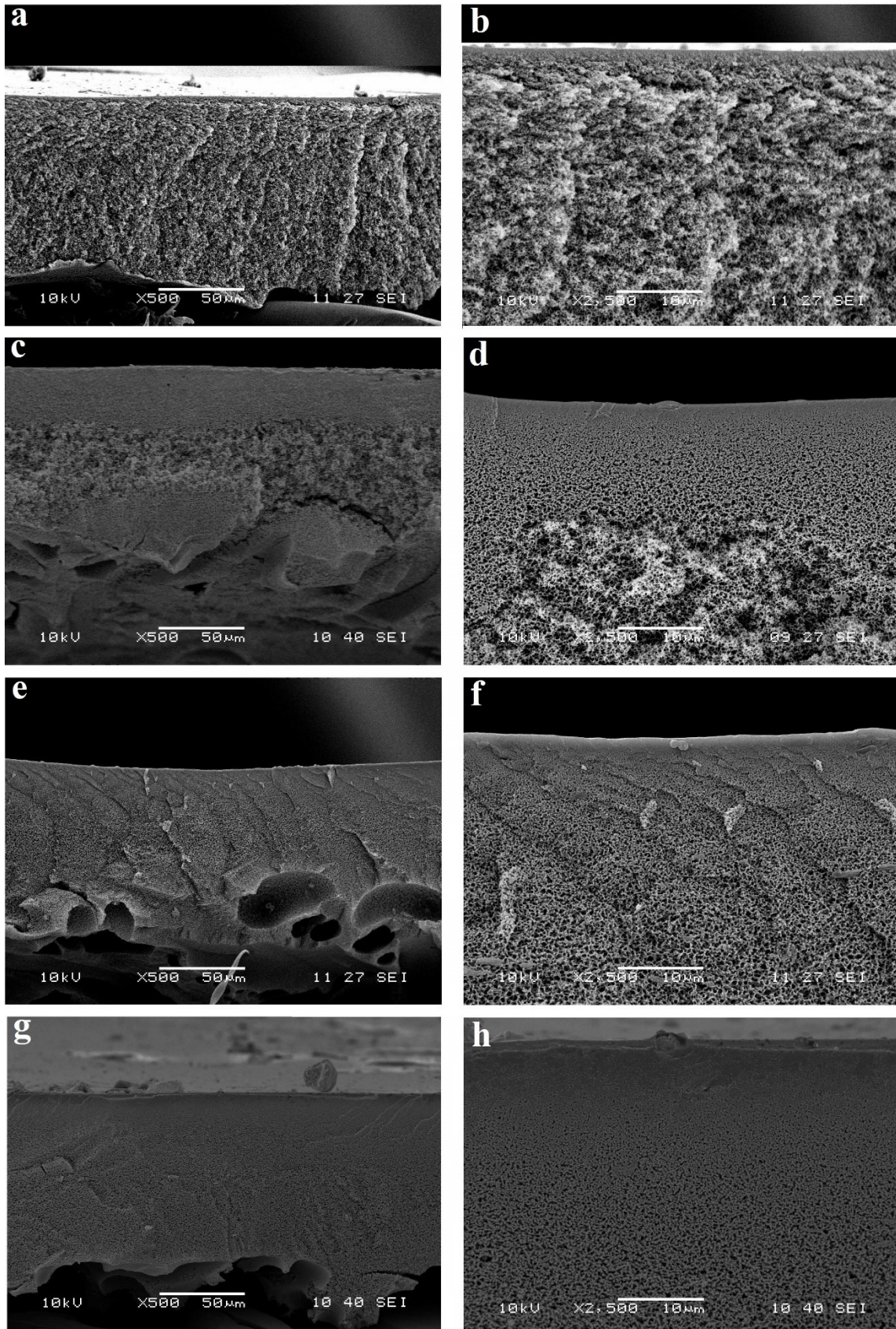
251 **Figure 2.** FTIR spectra for untreated and 120°C 3h heat treated PANI-PAMPSA membranes

252 3.2. SEM and AFM analysis

253 The cross-section and surface SEM images of the membranes are shown in Figure 3 and 4,
254 respectively.

255

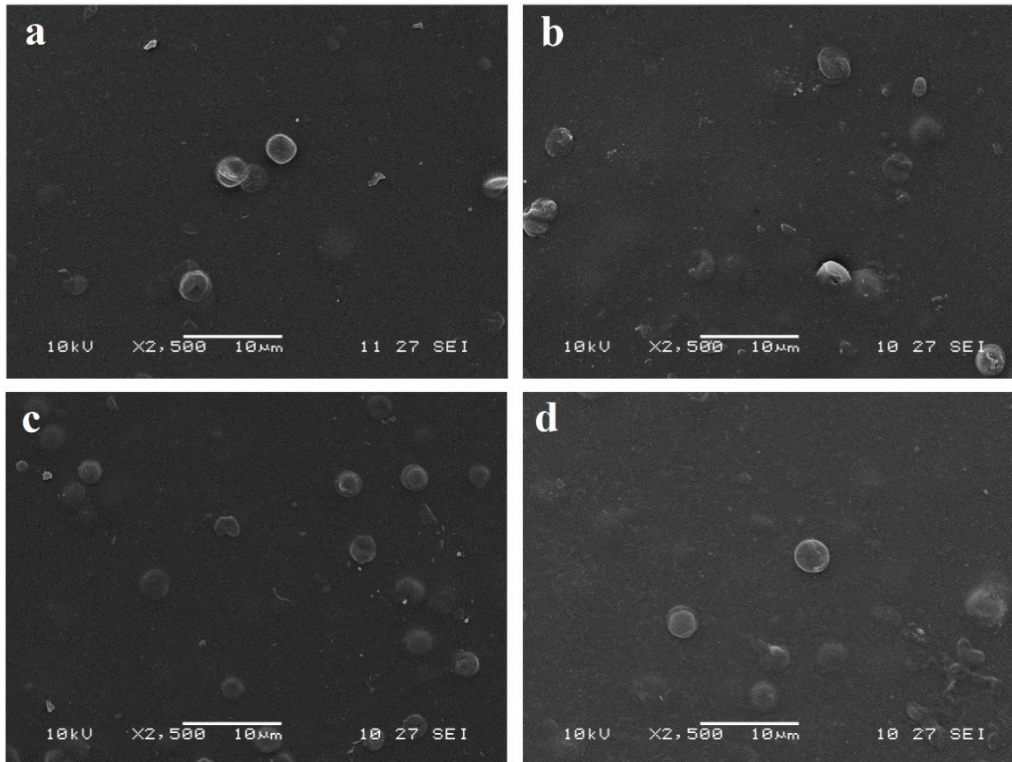
256



257

258 **Figure 3.** Cross-section SEM images of (a, b) Untreated, (c, d) 110°C 1h, (e, f) 120°C 1h, (g,
 259 h) 120°C 3h heat treated PANI-PAMPSA membranes with two different magnifications.

260



261

262

263

264

Figure 4. Surface SEM images of (a) Untreated, (b) 110°C 1h, (c) 120°C 1h, (d) 120°C 3h heat treated PANI-PAMPSA membranes

265

266

267

268

269

270

271

272

273

Fig. 3 shows that the cross-section of the untreated PANI-PAMPSA has an asymmetric structure, with relatively dense but still porous thin top layer and a more porous spongy layer underneath. With the heat treatment process the membrane became denser (Fig 3b-d) and the pore sizes of the matrix decrease as the temperature increased. The top layer turned into a denser layer, and furthermore, the thickness of the dense top layer appeared to increase with the increasing temperature. These changes, especially to the top layer, will play an important role in MWCO of the membranes because the separation takes place at the top layer of the membrane. This is in line with the results obtained by other researchers [27, 57] that showed that increasing the temperature increased the density of the top layer.

274

275

276

277

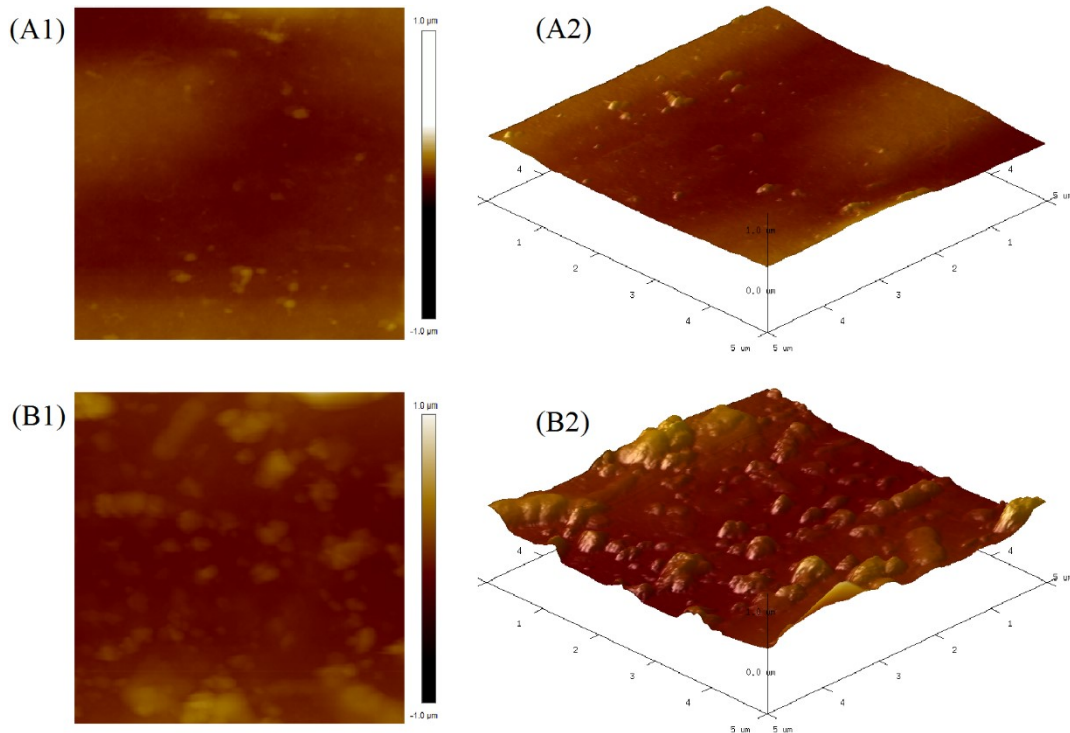
Figure 4 shows that both untreated and heat treated membranes present surface structures with randomly distributed, drop-like, round shape and similar-sized bulges. The heat treated membrane have a larger number of bulges, but there is no observable pin holes or deformations etc. on the surfaces on either of the membranes.

278

279

Since no difference was observed in membrane surfaces using SEM imaging, AFM was used to identify if there were any differences in the surface roughness between the untreated and

280 heat treated membrane. Figure 5 shows the 2D and 3D AFM images of the PANI-PAMPSA
281 membranes untreated and 120 °C 3h heat treated membrane as a representative sample. Table
282 2 show roughness values (mean roughness, R_a and root mean square roughness, R_q).



283

284

285

Figure 5. AFM images of PANI-PAMPSA membranes
(A1 and A2 untreated, B1 and B2 120°C 3h heat treated)

286 Figure 5 shows that the surface of the untreated membrane is quite smooth and that after the
287 heat treatment, the surface became rough. The observed increase in roughness can be attributed
288 to the formation of a mesoscopic structure associated with agglomeration of polymer chains
289 [49] and the degradation of the surface at that temperature [48]. Evaporating the residual
290 solvent or trap gases may have contributed to the formation of these island type structures on
291 the surface [49]. The increase of surface roughness of the membrane after heat treatment was
292 further confirmed by the surface roughness parameters in Table 2. The R_a and R_q values are
293 29.0 and 34.1 nm for untreated membrane and they increased significantly to 79.6 and 105 nm
294 after heat treated process. The results are in line with other studies that reported an increase in
295 surface roughness of PANI [49] and polyethersulfone [48] membranes on heat treatment.

296

297

298 **Table 2.** Some roughness values for PANI-PAMPSA membranes

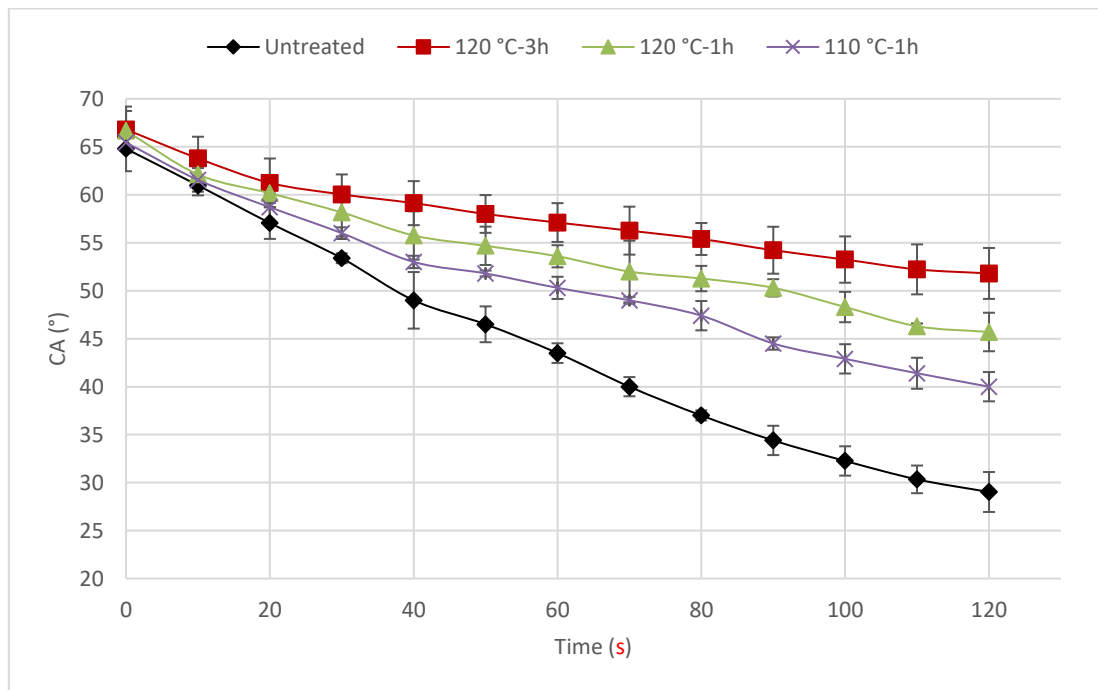
Membrane	Ra (nm)	Rq (nm)
Untreated	29.0	34.1
120°C 3h heat treated	79.6	105

299

300 **3.3. Dynamic contact angle analysis**

301 Dynamic contact angle analysis was performed to evaluate the surface wettability rate and
 302 roughness of the prepared membranes. Dynamic contact angle results for untreated and heat
 303 treated membranes are given in Figure 6. The contact angle pictures at the start and end point
 304 obtained in 2 minutes for untreated and 120 °C 3h heat treated PANI-PAMPSA membranes
 305 are shown in Figure 7.

306

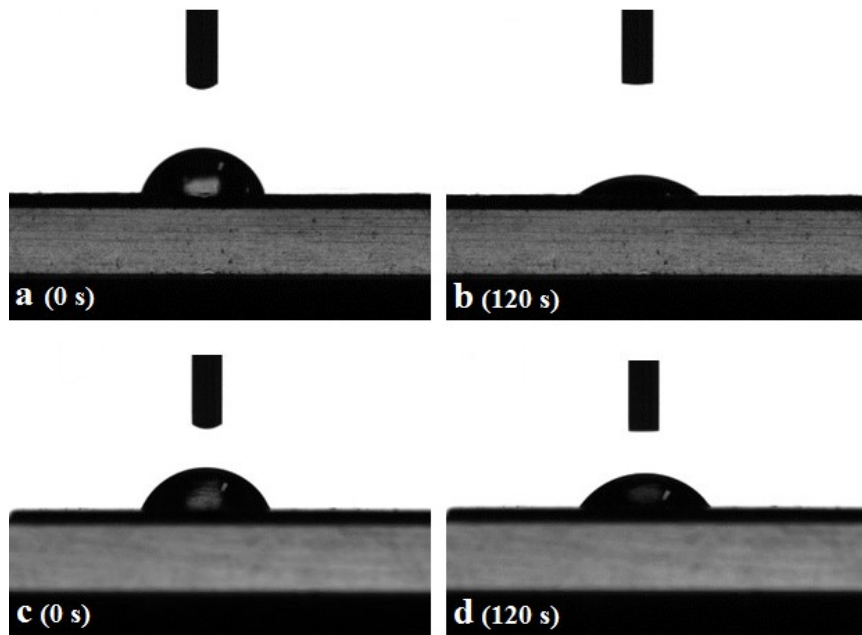


307

308 **Figure 6.** Dynamic contact angle results of a selection of PANI-PAMPSA membranes

309

310



311

312 **Figure 7.** Contact angle pictures of PANI-PAMPSA membranes at the start (0 Second) and
 313 end point (120 second). (a, b) Untreated, (c, d) 120°C 3h heat treated PANI- PAMPSA
 314

315

316 It can be observed in Figures 6 and 7 that contact angles of untreated and 120°C 3h heat treated
 317 PANI-PAMPSA membranes decreased from 65° to 29° and 67° to 52° in 2 minutes
 318 respectively. This shows that the main difference between the membranes is the reducing rate
 319 of the contact angle. The rate at which the contact angle decrease is higher for the untreated
 320 membranes, whereas the heat treated membranes show a slower reducing rate. Although the
 321 heat treated membranes do have a rougher surface, which should decrease the contact angle
 322 [50], they also have a more dense structure skin layer with smaller pores resulting in the
 323 droplets entering the pores slower. As determined by IR, heat treatment did not lead to any
 324 significant change in the chemical structure of the heat treated membranes, thus the
 325 hydrophilicity/hydrophobicity of the membranes is similar before and after the heat treatment.
 326 Therefore the results suggest that smaller pore size along with the shrunk and denser structure
 of the membrane skin layer lead to slower reducing rate of the contact angle.

327 3.4. Swelling and stability results

328 Table 3 shows the swelling degree (%) and stability (%) results obtained for the untreated and
 329 120 °C 3h heat treated membrane in different solvents.

330

331 **Table 3.** Stability and swelling degree results of the membranes in different solvents

Stability (Δ Weight) (%)	Swelling (%)
----------------------------------	--------------

Solvent	Untreated	120°C 3h treated	Untreated	120°C 3h treated
Water	0.81 ± 0.15	0.33 ± 0.02	115 ± 4.3	110 ± 2.8
Methanol	1.43 ± 0.10	0.66 ± 0.06	111 ± 5.2	90.5 ± 7.7
2-propanol	0.80 ± 0.17	0.32 ± 0.01	73.1 ± 2.5	71.4 ± 3.7
Acetone	1.00 ± 0.65	0.29 ± 0.01	88.9 ± 2.2	78.4 ± 6.7
Toluene	1.28 ± 0.56	0.65 ± 0.04	69.2 ± 0.35	48.9 ± 1.7
Hexane	0.48 ± 0.16	0.16 ± 0.01	22.9 ± 6.6	20.0 ± 3.0

332

333 The stability test results (after one week) (Table 3) show that the weight loss percentages for
334 both untreated and heat treated membranes are low in all tested solvents. For the heat treated
335 membrane, there was no significant difference of weight after one week for all tested solvents.
336 Furthermore, the filtration stability tests performed in 2-propanol, acetone and methanol for a
337 total filtration time of 24h (8h for each solvent) resulted in a total weight loss percentage of the
338 120 °C 3h heat treated membrane of 1.92%. This weight loss can be attributed to the removal
339 of unreacted chemicals (monomers etc.), low molecular weight PANI structures inside the
340 membrane bulk structure and the pores because of high pressure. Membrane filtration stability
341 was further confirmed during an eight hour pure solvent filtration study (Fig S1) and cross-
342 SEM images before and after the filtration (Fig S2). Fig. S1 show that the pure solvent
343 permeances for 8 hours of filtration (for each solvent) remained constant. If the membranes
344 were not stable, the permeance would increase due to the deformation/degradation of the
345 membrane structure. Fig. S2 show the cross-section SEM images of the 120 °C 3h heat treated
346 membrane before and after the filtration study. It can be observed that there is no significant
347 difference and no deformations on the membrane cross sectional structure after 8h of filtration,
348 further confirming the filtration stability of the heat treated membrane.

349 In order to investigate the interactions between the membranes and the solvents, swelling
350 studies (Table 3) were performed. The heat treated membrane swelled less than the untreated
351 membrane in all solvents, and the polarity of the solvents was directly related to the swelling
352 degrees of the membranes. Polarities of the solvents from low to high are in the order of:
353 hexane, toluene, 2-propanol, acetone, methanol and water. Due to the polar structure of the
354 PANI membrane, more polar solvents resulted in a higher swelling due to the stronger
355 interactions between the membrane and the solvent [51]. The highest swelling degree in
356 organic solvents was with methanol, this is because of the polarity (as per above) and H-

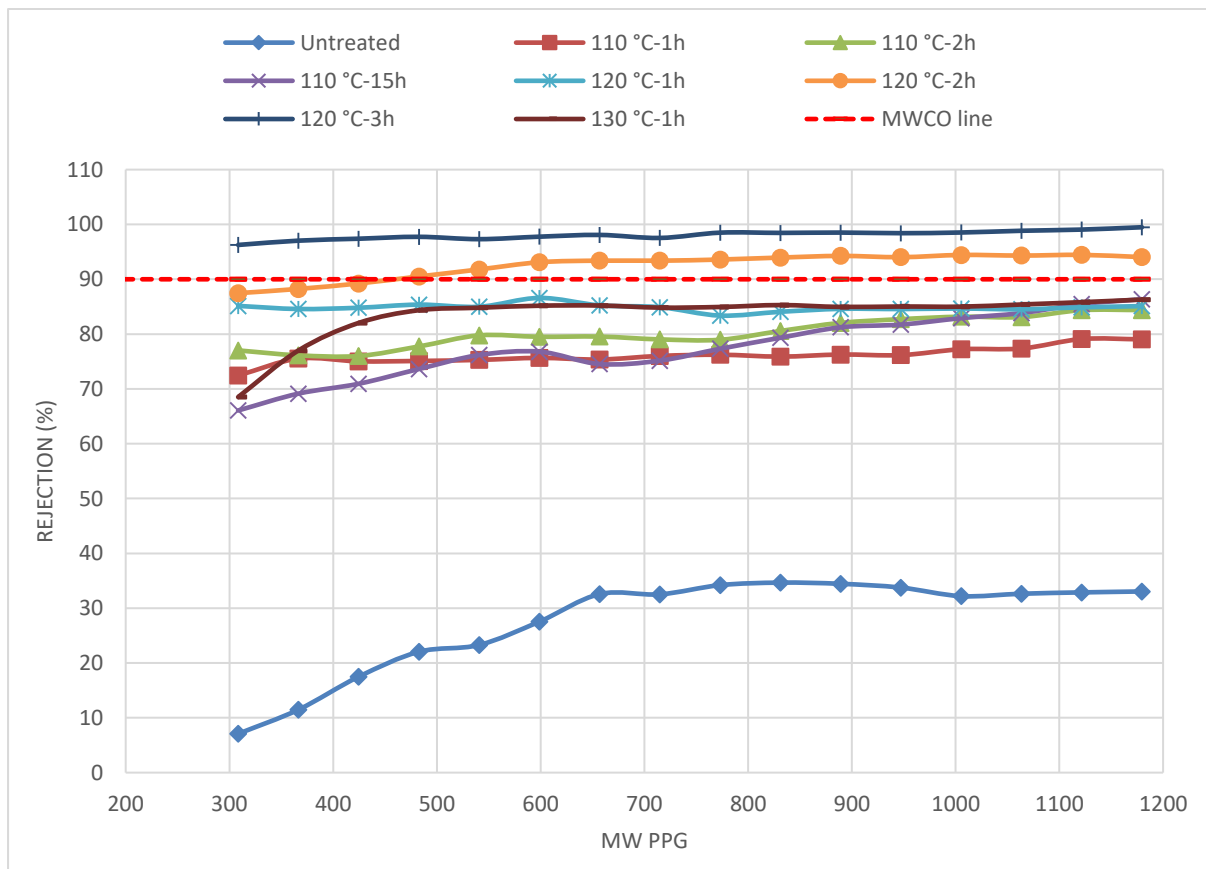
357 bonding properties [51] but it is also related to the size and shape of the solvents [27]. Methanol
358 is a small polar molecule that better interacts with the charged backbone of polyaniline [52].

359

360 3.5. Nanofiltration tests and MWCO determinations

361 Nanofiltration experiments were performed to investigate the rejection levels of the membranes
362 in different solvents by using different molecular weight of PPGs. The rejection results in 2-
363 propanol, acetone and methanol are shown in Figure 8, 9 and 10, respectively. Figure 11 shows
364 the rejection properties of the best membrane obtained, 120 °C 3h heat treatment in three
365 solvents.

366



367

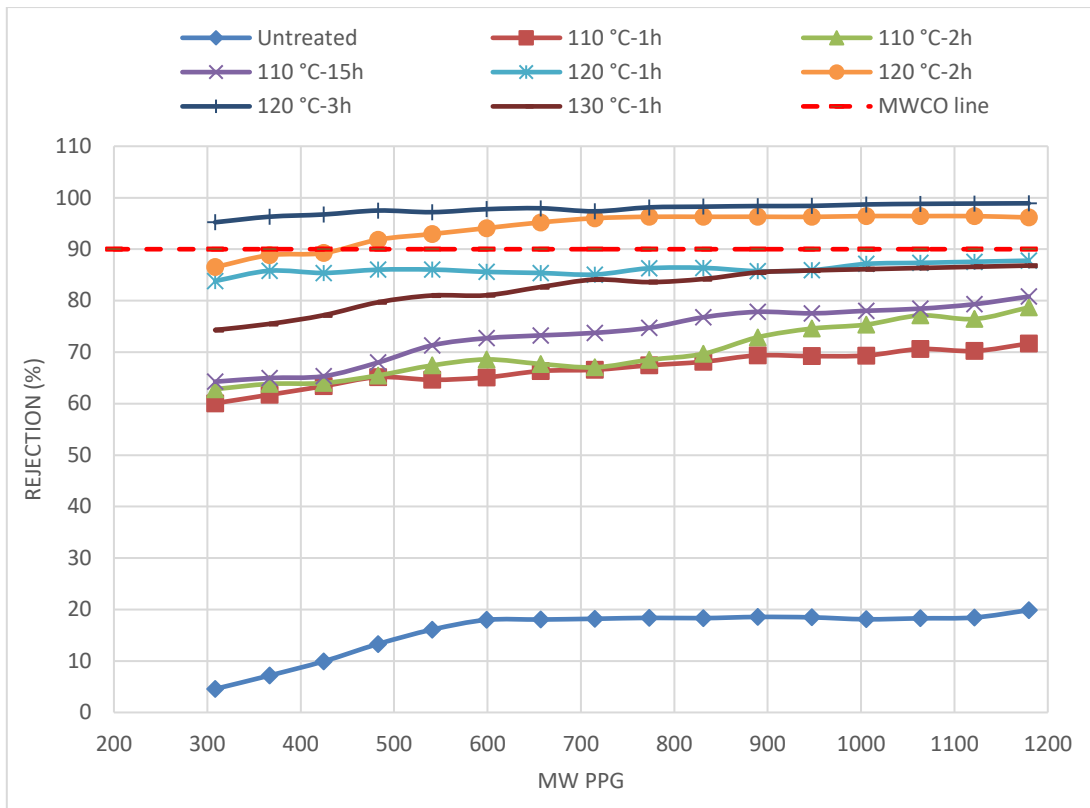
368

369 **Figure 8.** MWCO-curves of the membranes in 2-propanol

370

371

372

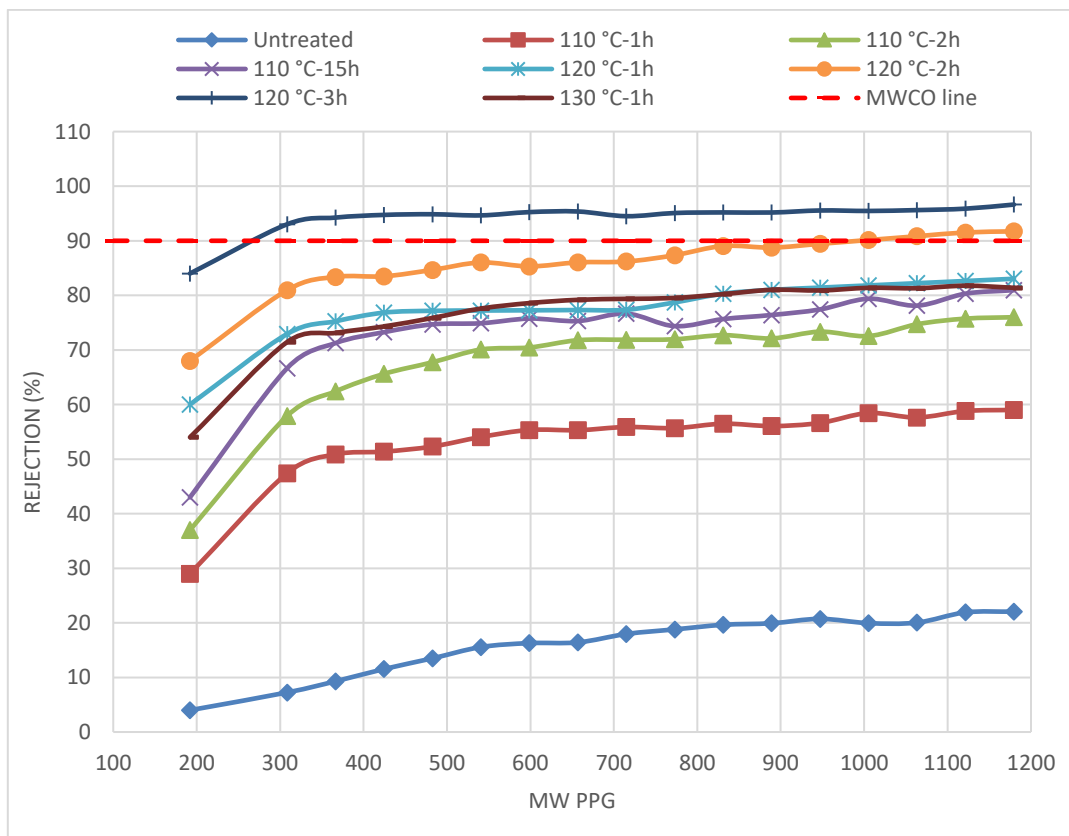


373

Figure 9. MWCO-curves of the membranes in Acetone

374

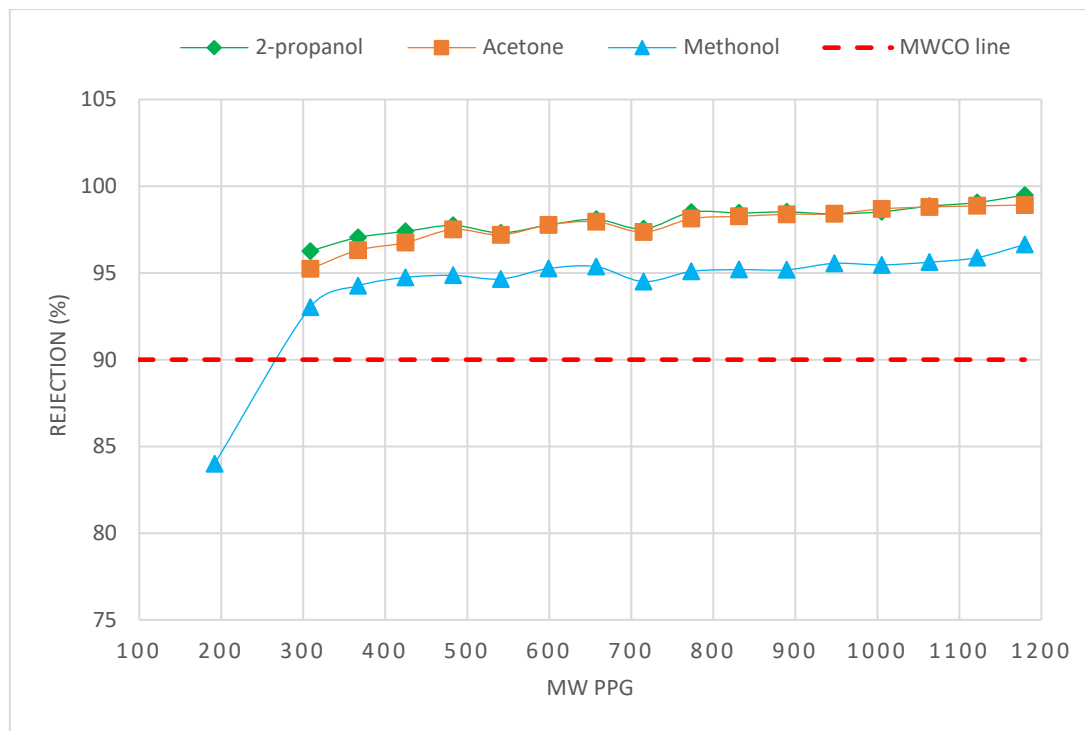
375



376

Figure 10. MWCO-curves of the membranes in Methanol

377



379

380

Figure 11. MWCO-curves of the 3h heat treated membrane in three solvents

381

382 In all solvents the best rejection was obtained for 120°C 3h heat treated PANI-PAMPSA
 383 membrane with a MWCOs lower than 300 Da. The exact MWCO values could not be
 384 determined for 2-propanol and acetone because there was no signal below 300 Da in these
 385 solvents (Figures 8 and 9). For the methanol results (Figures 10 and 11) there was a signal on
 386 192 Da related to tripropylene glycol so by using this signal the MWCO of the treated
 387 membrane could be determined as 266 Da.

388 On the other hand 120 °C 2h heat treated membrane showed MWCO of 480, 430 and 950 Da
 389 in 2-propanol, acetone and methanol, respectively. Except these 2 membranes, all other
 390 membranes have MWCO higher than 1200 Da although they are all having a lower MWCO
 391 than the untreated membrane in all solvents for all PPGs. Heat treatment at 130 °C decreased
 392 the rejection contrary to other temperatures. This can be attributed to the deformation of
 393 membrane support layer at this temperature. The melting temperature of PE/PP support is
 394 around 130 °C (especially polyethylene) [53] so it might have been damaged at 130 °C.

395 Figure 11 shows the rejection performance of the best membrane (120 °C 3h) in three solvents.
 396 It was observed that the rejection in 2-propanol and acetone are quite similar but higher than
 397 in methanol. This can be explained by considering the swelling degree of the membrane in
 398 different solvents (in Table 2) because the swelling of the membrane in methanol is higher than

399 the 2-propanol and acetone, owing to its higher polarity, H-bonding ability and smaller shape.
400 Higher swelling make the membrane pores relatively open, therefore the rejection ratio in
401 methanol is lower, although it still remain in the nanofiltration range. Contrary to the rejection
402 results, higher swelling degrees of the membranes increased the permeance of the solvents,
403 through the relatively opened pores, and the permeance results obtained for acetone, 2-propanol
404 and methanol were 0.46, 0.60 and 0.74 L m⁻² h⁻¹bar⁻¹, respectively. These results are similar
405 with other reported OSN studies [27, 34, 51, 54].

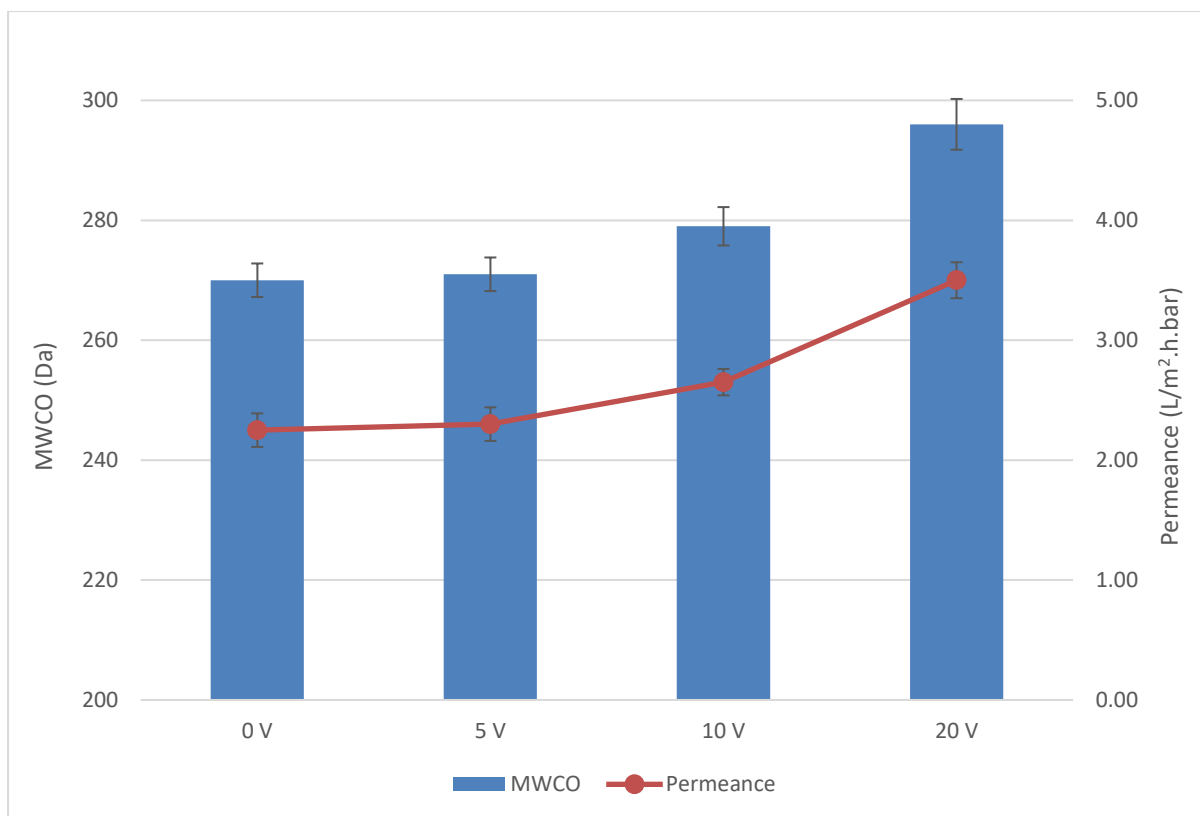
406

407 **3.6. Conductivity, cross-flow filtration and tuneability studies**

408 Conductivity measurements were performed to see if the PANI-PAMPSA membranes were
409 conductive and whether the heat treatment affects the conductivity. Conductivities of the
410 untreated and 120°C 3h heat treated membranes were 1.80x10⁻⁴ and 1.17x10⁻⁴ S.cm⁻¹,
411 respectively. This showed that both untreated and heat treated membranes are conductive and
412 that the heat treatment process did not cause a significant change in the conductivity. The slight
413 decrease of the conductivity after the heat treatment may be attributed to the poorer contact
414 between probe and membrane surface because of the higher surface roughness [55].

415 Cross-flow filtration studies were performed to compare the MWCO and permeance under
416 applied potential and to investigate the electrical tuneability of the 120°C 3h heat treated
417 membrane. Figure 12 shows the changes on the MWCOs and permeance for different applied
418 potentials (0, 5, 10, 20 V). For 5 V applied potential, there was no significant change in both
419 the permeance and MWCO because significant tuneability has previously only been observed
420 for potential with 7 V or more applied potential [32]. It was further observed that increasing
421 the applied potential from increased both the MWCOs and the permeance of the membrane
422 from 270 to 296 Da and 2.25 to 3.50 Lm⁻²h⁻¹ bar⁻¹, respectively. The main reason for this
423 increase in MWCO and permeance is likely due to the applied voltage providing extra charge
424 to the already positively charged PANI-PAMPSA membrane surface. Providing this additional
425 charge would increase the steric hindrance between the chain and thus compel the chains to
426 loosen or the pores to open slightly [56, 57]. Overall, these results show that this in-situ doped
427 and low temperature heat treated PANI-PAMPSA membranes show promise to be applied in
428 electrical tuneable separations in OSN.

429



430

431 **Figure 12.** MWCO and permeance values of 120 °C 3h heat treated membrane under applied
 432 potentials of 0, 5, 10 and 20 V

433

434 4. Conclusion

435 Novel PANI-PAMPSA OSN membranes with electrically tuneable properties were developed.
 436 Heat treatment, below the crosslinking temperature, was used to prepare in-filtration durable
 437 NF-membranes, without thermal crosslinking. Results showed that the heat treated PANI-
 438 PAMPSA membranes were stable in organic solvents with different polarities with no loss in
 439 performance after repeated use. Besides, IR spectra of both untreated and heat treated
 440 membranes confirmed the absence of any chemical alteration affecting the PANI-PAMPSA
 441 membranes, however SEM and AFM images indicated that the top skin layer of the heat treated
 442 membranes became more dense, with an increase in surface roughness. These results were
 443 supported by dynamic contact angle and filtration experiments. Dynamic contact angle
 444 measurements indicated that with the heat treatment, the surface pores became smaller, and
 445 consistently, the permeance decreased and the rejection increased. Filtration studies showed
 446 that the 120°C 3h heat treated PANI-PAMPSA membranes had NF range rejections with the
 447 MWCOs lower than 300 Da for all tested solvents (e.g., 266 Da in methanol). The conductivity

448 was successfully retained after the heat treatment, and the application of 20 V potential led to
449 an increase of 10.4 % and 55.6 % for MWCO and permeance of membrane, respectively.
450 Therefore, the prepared OSN membrane can be controlled in-situ by applying electrical
451 potential during the filtration process. In summary, we have for the first time developed durable
452 OSN membranes with electrical tuneability.

453 **Acknowledgement**

454 The authors acknowledge the financial support of the European Research Council (ERC)
455 Consolidator grant TUNEMEM (Project reference: 646769; funded under H2020-EU.1.1.-
456 EXCELLENT SCIENCE). Adem Sarihan thanks the “Scientific and Technological Research
457 Council of Turkey (TUBITAK) BIDEB-2219 International Postdoctoral Research Fellowship
458 Programme” for financial support. The authors thank the technician team at the Departments
459 of Chemical Engineering and Physics, University of Bath for technical support.

460

461 **References**

462

463 [1] M. Bastin, K. Hendrix, I. Vankelecom, Solvent resistant nanofiltration for acetonitrile based
464 feeds: A membrane screening, *Journal of Membrane Science*, 536 (2017) 176-185.

465

466 [2] Y. Feng, M. Weber, C. Maletzko, T-S. Chung, Facile fabrication of sulfonated
467 polyphenylenesulfone (sPPSU) membranes with high separation performance for organic
468 solvent nanofiltration, *Journal of Membrane Science*, 549 (2018) 550-558.

469

470 [3] Y.H. See-Toh, M. Silva, A. Livingston, Controlling molecular weight cut-off curves for
471 highly solvent stable organic solvent nanofiltration (OSN) membranes, *Journal of Membrane
472 Science*, 324 (2008) 220-232

473

474 [4] M. Amirilargani, M. Sadrzadeh, E.J.R. Sudhölter, L.C.P.M. de Smet, Surface modification
475 methods of organic solvent nanofiltration membranes, *Chemical Engineering Journal*, 289
476 (2016) 562-582.

477

478 [5] S. Hermans, H. Marien, C.V. Goethem, I.F.J Vankelecom, Recent developments in thin
479 film (nano)composite membranes for solvent resistant nanofiltration, *Current Opinion in
480 Chemical Engineering*, (2015) 8 45-54.

481

482 [6] F. Yuan, Y. Yang, R. Wang, D. Chen, Poly(vinylidene fluoride) grafted polystyrene
483 (PVDF-g-PS) membrane based on in situ polymerization for solvent resistant nanofiltration,
484 *RSC Adv.* (2017) 7 33201.

485

486 [7] A.V. Volkov, G.A. Korneeva, G.F. Tereshchenko, Organic solvent nanofiltration: prospects
487 and application, *Russian Chemical Reviews*, 77 (11) (2008) 983-993.

488
489 [8] A.R.S. Teixeira, J.L.C. Santos, J.G. Crespo, Solvent resistant diananofiltration for
490 production of steryl esters enriched extracts, *Separation and Purification Technology*, 135
491 (2014) 243-251.
492
493 [9] D. Peshev, L.G. Peeva, G. Peeva, I.I.R. Baptista, A.T. Boam, Application of organic solvent
494 nanofiltration for concentration of antioxidant extracts of rosemary (*Rosmarinus officinalis* L.),
495 *Chemical engineering research and design*, 89 (2011) 318-327.
496
497 [10] R. Valadez-Blanco, F.C. Ferreira, R.F. Jorge, A.G. Livingston, A membrane bioreactor
498 for biotransformations of hydrophobic molecules using organic solvent nanofiltration (OSN)
499 membranes, *Journal of Membrane Science*, 317 (2008) 50-64.
500
501 [11] F.C. Ferreira, H. Macedo, U. Cocchini, A.G. Livingston, Development of a Liquid-Phase
502 Process for Recycling Resolving Agents within Diastereomeric Resolutions, *Organic Process*
503 *Research & Development*, (2006) 10 784-793
504
505 [12] G. Székely, J. Bandarra, W. Heggie, B. Sellergren, F. C. Ferreira, Organic solvent
506 nanofiltration: A platform for removal of genotoxins from active pharmaceutical ingredients,
507 *Journal of Membrane Science*, 381 (2011) 21-33.
508
509 [13] R. Abejon, A. Garea, A. Irabien, Analysis and Optimization of Continuous Organic
510 Solvent Nanofiltration by Membrane Cascade for Pharmaceutical Separation, *American*
511 *Institute of Chemical Engineers*, 60 3 (2014) 931-948.
512
513 [14] L.S. White, C.R. Wildemuth, Aromatics Enrichment in Refinery Streams Using
514 Hyperfiltration, *Ind. Eng. Chem. Res.*, 45 (2006) 9136-9143.
515
516 [15] L.S. White, Development of large-scale applications in organic solvent nanofiltration and
517 pervaporation for chemical and refining processes, *Journal of Membrane Science*, 286 (2006)
518 26-35.
519
520 [16] D. Roy, J.N. Cambre, B.S. Sumerlin, Future perspectives and recent advances in stimuli-
521 responsive materials, *Progress in Polymer Science*, 35 (2010) 278-301.
522
523 [17] H.H. Himsedt, K.M. Marshall, S.R. Wickramasinghe, pH-responsive nanofiltration
524 membranes by surface modification, *Journal of Membrane Science*, 366 (2011) 373-381.
525
526 [18] M.A.C. Stuart, W.T.S.Huck, J. Genzer, M. Muller, C. Ober, M. Stamm, G.B. Sukhurokov,
527 I. Szlifier, V.V. Tsukruk, M. Urban, F. Winnik, Z. Sauscher, I. Luzinow, S. Minko, Emerging
528 applications of stimuli-responsive polymer materials, *Nature materials*, 9 (2010) 101-113.
529
530 [19] O. Azzaroni, UCST wetting transitions of polyzwitterionic brushes driven by self-
531 association, *Angewandte Chemie*, 118 (2006) 1802-1806.
532
533 [20] A.G. Skirtach. A.M. Javier, O. Kreft, K. Kohler, A.P. Alberola, H. Mohvald, W.J. Parak,
534 G.B. Sukhurokov, Laser-Induced Release of Encapsulated Materials inside Living Cells,
535 *Angewandte Chemie*, 45 (2006) 4612-4617.
536

- 537 [21] C. Weidlich, K-M. Mangold, Electrochemically switchable polypyrrole coated membranes,
538 *Electrochimica acta*, 56 (2011) 3481-3484.
539
- 540 [22] L. Xu, S. Shahid, A.K. Holda, E.A.C. Emanuelsson, Stimuli responsive conductive
541 polyaniline membrane: In-filtration electrical tuneability of flux and MWCO, *Journal of*
542 *Membrane Science*, 552 (2018) 153-166.
543
- 544 [23] M.R. Anderson, B.R. Mattes, H. Reiss, R.B. Kaner, Gas Separation Membranes: A Novel
545 Application for Conducting Polymers, *Synthetic Metals*, 41-43 (1991) 1151-1154.
546
- 547 [24] P.C. Rodrigues, G. P. de Souza, J.D.D.M. Neto, L. Akcelrud, Thermal treatment and
548 dynamic mechanical thermal properties of polyaniline, *Polymer*, 43 (2002) 5493-5499.
549
- 550 [25] W. Hu, S. Chen, Z. Yang, L. Liu, H. Wang, Flexible Electrically Conductive
551 Nanocomposite Membrane Based on Bacterial Cellulose and Polyaniline, *J. Phys. Chem. B.*,
552 (2011) 115 8453-8457.
553
- 554 [26] P. Rannou, M. Nechtschein, J.P. Travers, D. Bernera, A. Walter, D. Djurado, Ageing of
555 PANI: chemical, structural and transport consequences, *Synthetic Metals*, 101 (1999) 734-737.
556
- 557 [27] M. Sairam, X.X. Loh, K. Li, A. Bismarck, J.H.G. Steinke, A.G. Livingston, Nanoporous
558 asymmetric polyaniline films for filtration of organic solvents, *Journal of Membrane Science*,
559 330 (2009) 166-174.
560
- 561 [28] Z. Fan, Z. Wang, M. Duan, J. Wang, S. Wang, Preparation and characterization of
562 polyaniline/polysulfone nanocomposite ultrafiltration membrane, *Journal of Membrane*
563 *Science*, 310 (2008) 402-408.
564
- 565 [29] J. Pellegrino, The Use of Conducting Polymers in Membrane-Based Separations, *Annals*
566 *New York academy of sciences*, 984 (2003) 289-305.
567
- 568 [30] H. Hu, J.L. Cadenas, J.M. Saniger, P.K. Nair, Electrically Conducting Polyaniline-
569 Poly(acrylic acid) Blends, *Polymer International*, 45 (1998) 262-270.
570
- 571 [31] L. Xu, Electrically Tuneable Membranes: Revolutionising Separation and Fouling Control
572 for Membrane Reactors, PhD theses, University of Bath, (2016).
573
- 574 [32] R. Rohani, Linking the Microstructural and Separation Properties of Electrically Tuneable
575 Polyaniline Pressure Filtration Membranes, MSc thesis, The University of Auckland, (2013).
576
- 577 [33] X.X. Loh, M. Sairam, A. Bismarck, J.H.G. Steinke, A.G. Livingston, K. Li, Crosslinked
578 integrally skinned asymmetric polyaniline membranes for use in organic solvents, *Journal of*
579 *Membrane Science*, 326 (2009) 635-642.
580
- 581 [34] X.X. Loh, M. Sairam, A. Bismarck, J.H.G. Steinke, A.G. Livingston, K. Li, Polyaniline
582 hollow fibres for organic solvent nanofiltration , *Chem. Commun*, (2008) 6324-6326.
583
- 584 [35] J. Lin, Q. Tang, J. Wu, H. Sun, Synthesis, characterization and properties of
585 polyaniline/expanded vermiculite intercalated nanocomposite, *Sci. Technol. Adv. Mater.*, 9
586 (2008) 025010.

587
588 [36] S. Moon, Y.H. Jung, D.K. Kim, Enhanced electrochemical performance of a crosslinked
589 polyaniline coated graphene oxide-sulfur composite for rechargeable lithium sulfur batteries,
590 *Journal of Power Sources*, 294 (2015) 386-392.
591
592 [37] X. Wang, D. Liu, J. Deng, X. Duan, J. Guo, P. Liu, Improving cyclic stability of
593 polyaniline by thermal crosslinking as electrode materials for supercapacitor, *RSC Adv.*, 5
594 (2015) 5 78545.
595
596 [38] C-H. Chen, Thermal and Morphological Studies of Chemically Prepared Emeraldine-
597 Base-Form Polyaniline Powder, *Journal of Applied Polymer Science*, 89 (2003) 2142-2148.
598
599 [39] J.A. Conklin, S-C. Huang, S-M. Huang, T. Wen, R.B. Kaner, Thermal Properties of
600 Polyaniline and Poly(aniline-co-o-ethylaniline), *Macromolecules*, 28 (1995) 6522-6527.
601
602 [40] J. Shen, S. Shahid, A. Sarihan, D.A. Patterson, E.A.C. Emanuelsson, Effect of polyacid
603 dopants on the performance of polyaniline membranes inorganic solvent Nanofiltration,
604 *Separation and Purification Technology*, 204 (2018) 336-344
605
606 [41] Y.S. Kang, H.J. Kim, U.Y. Kim, Asymmetric membrane formation via immersion
607 precipitation method. I. Kinetic effect, *Journal of Membrane Science*, 60 (1991) 219-232.
608
609 [42] R. Rohani, M. Hyland, D. Patterson, A refined one-filtration method for aqueous based
610 nanofiltration and ultrafiltration membrane molecular weight cut-off determination using
611 polyethylene glycols, *Journal of Membrane Science*, 382 (2011) 278-290.
612
613 [43] C.J. Davey, Z.X. Low, R.H. Wirawan, D.A. Patterson, Molecular weight cut-off
614 determination of organic solvent nanofiltration membranes using poly(propylene glycol),
615 *Journal of Membrane Science*, 526 (2017) 221-228.
616
617 [44] S.J. Kim, N.R. Lee, B.J. Yi, S.I. Kim, Synthesis and Characterization of Polymeric
618 Acid-Doped Polyaniline Interpenetrating Polymer Networks, *Journal of Macromolecular
619 Science*, Part A: Pure and Applied Chemistry, 43 (2006) 497-505.
620
621 [45] L. Hechavarria, H. Hu, M.E. Rincon, Polyaniline-poly(2-acrylamido-2-methyl-1-
622 propanosulfonic acid) composite thin films: structure and properties, *Thin Solid Films*, 441
623 (2003) 56-62.
624
625 [46] A.G. Willis, S. Haron, Synthesis and characterization of composite polyaniline as
626 hydrogen gas detector, *Malaysian Journal of Fundamental and Applied Sciences*, 13 4 (2017)
627 559-562.
628
629 [47] A.J. Milton, A.P. Monkman, A comparative study of polyaniline films using thermal
630 analyses and IR spectroscopy, *J. Phys. D: Appl. Phys.* 26 (1993) 1468.
631
632 [48] A. Idris, N.M. Zain, Effect of Heat Treatment on The Performance and Structural Details
633 of Polyethersulfone Ultrafiltration Membranes, *Jurnal Teknologi*, 44 (F) (2006) 27-40.
634

- 635 [49] A. Bahramian, The effect of heat treatment on the surface structure of polyaniline
636 nanostructured film: An experimental and molecular dynamics approach, *Applied Surface*
637 *Science*, 311 (2014) 508-520.
638
- 639 [50] S-H. Yoon, *Membrane Bioreactor Processes: Principles and applications*, June 23, (2015)
640 CRC Press, ISBN 9781482255836.
641
- 642 [51] A. Rahy, T. Rguig, S.J. Cho, C.E. Bunker, D.J. Yang, Polar solvent soluble and hydrogen
643 absorbing polyaniline nanofibers, *Synthetic Metals*, 161 (2011) 280-284.
644
- 645 [52] D. Ballal, W.G. Chapman, Hydrophobic and hydrophilic interactions in aqueous mixtures
646 of alcohols at a hydrophobic surface, *The Journal of Chemical Physics* 139 (2013) 114706.
647
- 648 [53] M. Polaskova, R. Cermak, T. Sedlacek, J. Kalus, M. Obadal, P. SAha, Extrusion of
649 Polyethylene/Polypropylene Blends with Microfibrillar-Phase Morphology, *Polymer*
650 *composites*, (2010) 1427-1433.
651
- 652 [54] M. Sairam, X.X. Loh, Y. Bhole, I. Sereewatthanawut, K. Li, A. Bismark, J.H.G. Steinke,
653 A.G. Livingston, Spiral-wound polyaniline membrane modules for organic solvent
654 nanofiltration (OSN), *Journal of Membrane Science*, 349 (2010) 123-129.
655
- 656 [55] A. Lodha, S.M. Kilbey II, P.C. Ramamurthy, R.V. Gregory, Effect of annealing on
657 electrical conductivity and morphology of polyaniline films, *Journal of Applied Polymer*
658 *Science*, 82 (2001) 3602-3610.
659
- 660 [56] P.L. Donald, A.C. Hillier, Electrochemically modulated transport through a conducting
661 polymer membrane, *Journal of Membrane Science*, 208 (2002) 119-131.
662
- 663 [57] D.L.Pile, Y. Zhang, A.C. Hillier, Electrochemically Modulated Permeability of
664 Poly(aniline) and Composite Poly(aniline)-Poly(styrenesulfonate) Membranes, *Langmuir* 22
665 (2006) 5925-5931.